

# An Agent-Based Simulation Using Extensive Real Datasets: the Case of COVID-19 in Catalonia

M. Bosman<sup>1,\*</sup>, Y. Cordon<sup>1</sup>, M. Duran<sup>1</sup>, L. Gabbanelli<sup>1</sup>, C. García-Pérez<sup>2,3</sup>, X. Jordan<sup>4</sup>, M. Manera<sup>1,5</sup>, P. Masjuan<sup>1,6</sup>, A. Medina<sup>7</sup>, LI.M. Mir<sup>1</sup>, A. Oròs<sup>1</sup>, and V. Vitagliano<sup>2,3</sup>

<sup>1</sup>Institut de Física d'Altes Energies (IFAE), The Barcelona Institute of Science and Technology, Barcelona, Spain

<sup>2</sup>DIME, University of Genova, via all'Opera Pia 15, 16145 Genova, Italy

<sup>3</sup>INFN, Sezione di Genova, via Dodecaneso 33, 16146 Genova, Italy

<sup>4</sup>i2CAT Foundation, Edifici Nexus (Campus Nord UPC), Barcelona, Spain

<sup>5</sup>Serra Hünter Fellow, Departament de Física, Universitat Autònoma de Barcelona, Bellaterra, Spain

<sup>6</sup>Departament de Física, Universitat Autònoma de Barcelona, Bellaterra, Spain

<sup>7</sup>Centre d'Estudis Demogràfics (CED-CERCA), Barcelona, Spain

\*bosman@ifae.es

## ABSTRACT

During the COVID-19 pandemic, effective public policy interventions have been crucial in combating virus transmission, sparking extensive debate on crisis management strategies and emphasizing the necessity for reliable models to inform governmental decisions, particularly at the local level. Leveraging disaggregated socio-demographic microdata, including social determinants, age-specific strata, and mobility patterns, we design a comprehensive network model of Catalonia's population and, through numerical simulation, assess its response to the outbreak of COVID-19 over the two-year period 2020-21. Our findings underscore the critical importance of timely implementation of broad non-pharmaceutical measures and effective vaccination campaigns in curbing virus spread; in addition, the identification of high-risk groups and their corresponding maps of connections within the network paves the way for tailored and more impactful interventions.

*Keywords:* COVID-19, agent-based model, disease propagation, vaccine, Catalonia

## Introduction

The COVID-19 outbreak shed light on the critical role of timely and well-informed policy decisions in managing and mitigating the spread of infectious diseases. The challenge that policymakers have to face in an interconnected, global society is to find the correct balance between the economic and social impacts, together with psychological implications, of various interventions and public health considerations. Policies need to be adaptive, responding to quickly changing circumstances and emerging information. In this context, the significance of highly customizable simulations of epidemic models becomes evident: they provide not only valuable insights about the outbreak dynamics but also a versatile platform to promptly test scenarios in which different explicit containment measures (e.g., selective lockdowns, restrictions on specific mobility patterns, group-oriented vaccination campaigns) are put in place.

Mathematical modelling of sophisticated social environments can be consistently achieved within the framework of *agent-based models* (ABMs), computational models that simulate the emergent behaviour of complex networks starting from the structure of the interactions between the individual entities (the *agents*) of the system. Agents behave and interact with other agents and the environment in certain ways that would produce emerging effects that may differ from the effects of individuals. Concerning public health, this can be intuitively understood as the study of the spread of a certain disease – or, more in general, of unhealthy behaviours – in a community as a result of the demographic characteristics of single individuals and their social relations. The (abstract) control of the behaviour of each agent allows the evaluation of the response of the network to a given change and a relatively simple playground to identify the groups, or the links in the social network, where interventions could have the greatest impact<sup>1</sup>.

Epidemic ABMs can in principle provide a set of solution-focused tools to single out the most effective among various containment strategies. However, the robustness of the outcome of a simulation compared with the real spatiotemporal evolution of a disease is tightly entangled with the quality and volume of available socio-demographic data. To be realistic, the ABM-based simulation should rely on a network whose characteristics and properties reproduce, as closely as possible, the actual population. This implies having access to up-to-date granular repositories with high-resolution individual data, which,

39 unfortunately, are not always available, rarely ready-made, and seldom public. Socio-demographic data provides a snapshot of  
40 the substratum in which the disease may propagate. The disease itself with its bio-medical characteristics plays as well a key  
41 role. This information must be incorporated in any attempt to spread modelling.

42 In this paper, we use *real, disaggregated census and mobility data* of the population of Catalonia with its ~8M people to  
43 build a network model and simulate the sequence of events that characterised the natural history of COVID-19 in Catalonia. To  
44 the best of our knowledge, our census dataset (including over 120 socio-demographic variables for a representative sample of  
45 600k single agents in Catalonia) is one of the largest, raw datasets ever used to this scope.

46 The COVID-19 pandemic unfolded across the globe in early 2020, creating widespread disruptions in our societies. Many  
47 countries faced recurring waves of the virus, particularly intense in the initial two to three years. Stringent initial lockdown  
48 measures were followed by extensive vaccination campaigns that, together with the evolution of the virus into less deathly  
49 variants helped in restoring the situation to a level manageable by national health systems. Nevertheless, even four years later,  
50 new strains of the virus continue to circulate, posing ongoing challenges. Our time scope, which includes years 2020 and  
51 2021, did not require us to consider evolving viruses and multi-strain overlapping waves, but ABMs allow relatively easy  
52 implementation of such an effect when necessary.

53 In a first paper<sup>2</sup>, we focused on the province of Barcelona, employing an ABM to track the contagion that originated from a  
54 small set of randomly chosen infected individuals in early 2020. Residence location, household structure, employment situation,  
55 and mobility routines, along with the resulting pattern of contacts, including incidental contacts such as those arising in public  
56 transportation or due to increased social activities during holidays, were inferred from detailed, disaggregated census data  
57 and information supplied by mobile network operators. The evolution of the disease in the host and its intensity were taken  
58 to be age-dependent and modelled according to the first observations available at the time. In the first phase of our work, we  
59 successfully reproduced the curve of diagnosed cases in 2020, highlighting the distinct characteristics of the two main waves  
60 based on individuals' age and place of residence.

61 In the current simulation, *covering both 2020 and 2021 across all four provinces of Catalonia*, several improvements and  
62 additional features have been introduced. Notable enhancements include accounting for the impact of vaccination campaigns  
63 with different vaccines and a strongly age-dependent vaccination timeline. The wave patterns as revealed by epidemiological  
64 data varied among provinces due to differences in mobility, contacts, and the presence of distinct population groups affecting  
65 the disease propagation. Health personnel, residents in long-term care facilities, and workers in nursing homes have been  
66 treated separately given their roles during the outbreak. With these refinements, we have been able to simulate the five waves  
67 that occurred in 2020-21; we underscored the pivotal roles of lockdown measures and the vaccination campaign in controlling  
68 the pandemic and delved into the potential impact of different vaccine characteristics and vaccination timelines.

## 69 **Methods**

70 The Basic Health Area (known as Àrea Bàsica de Salut, or ABS, in Catalan) serves as the fundamental territorial unit used by  
71 the Catalan Health Department for the organization of primary healthcare services in Catalonia<sup>3</sup>. Typically, each ABS caters to  
72 approximately 20,000 individuals and is linked to its respective network of hospitals and health proximity centres. Catalonia  
73 is home to 374 such areas, distributed across its four provinces, as depicted in Figure 1. The demarcation of these areas is  
74 influenced by a combination of factors, including geography, demographics, and social dynamics. Notably, close to major cities,  
75 especially Barcelona, ABS areas tend to be more compact with a higher population density.

76 By integrating census data aggregated at the ABS level and daily mobility information between ABSs, we constructed a  
77 comprehensive model capturing realistic patterns of contacts and movements related to both work/school and social activities  
78 for the entire population. Healthcare system data on the daily counts of COVID-19 cases are used to calibrate our simulation.  
79 Information on the extensive vaccination campaign against COVID-19 launched in 2021 is also included.

## 80 **Census data**

81 The “Cens de Població”, or population census, which provides socio-demographic information by categorizing the Catalan  
82 territory into 5,107 census sections, was made available upon request by the Spanish National Statistics Institute (Instituto  
83 Nacional de Estadística, INE<sup>4</sup>). The latest available census (2011) contains detailed information on around 10% of the  
84 population, covering aspects such as housing, education, work, family structure, etc. Considering the effective weight of each  
85 of these individuals, the dataset yields insights into the 7,472,937 inhabitants of Catalonia at that time. The original 2011 set  
86 has been reorganized to match the ABS structure (see Section 1 of the Supplementary Material (SM) for further information).

87 The census used for population reconstruction lacks information on individuals aged 65 years and above residing in nursing  
88 facilities. To address this gap, we consulted the list of 1,002 official long-term care facilities established in 2019, incorporating  
89 details on available spaces therein<sup>5</sup>. The age distribution among the elderly residing in these facilities displays an almost  
90 symmetrically inverse pattern compared to those in family dwellings<sup>6</sup>. The oldest individuals among the elderly predominantly  
91 reside in residential care facilities, while the younger ones live in private homes. An additional segment was introduced into the

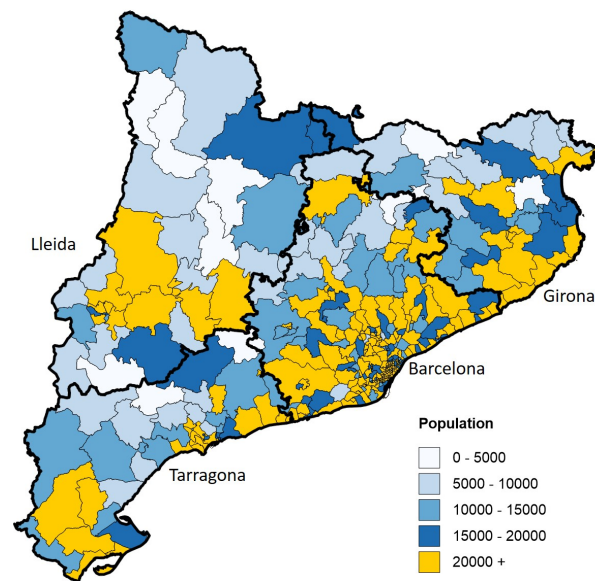


**Figure 1. Map of Catalan ABSs.** The map displays the 374 ABSs across the Catalan provinces of Barcelona, Girona, Lleida, and Tarragona (thick black lines); each ABS is depicted by a color code corresponding to its population size.

92 census file to accurately represent this specific demographic. Considering the average occupancy rate of nursing facilities at  
93 86%<sup>7</sup> and their respective locations, we reconstructed the demographic profile for an estimated population of 53,000 individuals  
94 residing in these homes. Ages were randomly assigned to individuals based on the overall age structure.

95 Additionally, during the summer season, Catalonia experiences an influx of temporary workers in the agricultural sector,  
96 with the province of Lleida hosting the largest proportion (see Section 1.2 in SM). We created an additional segment of the  
97 census file with over 4,000 temporary workers randomly assigned to mock farming companies. They reside in the same ABS as  
98 their workplace, share housing and are assigned social contacts like the rest of the population.

99 We devote special attention to two specific categories of sanitary workers (see Section 2.2 in SM). Sanitary workers engaged  
100 in geriatrics are estimated to be around 34,000, and sanitary workers operating in hospitals in close contact with infected  
101 patients at approximately 18,000.

## 102 Healthcare system data

103 We obtained comprehensive and anonymized data on the daily counts of COVID-19 cases, hospitalizations, intensive care  
104 unit (ICU) admissions, and deaths through the Program of Data Analysis for Research and Innovation in Health (“Programa  
105 d’Analítica de Dades per a la Recerca i la Innovació en Salut”, PADRIS<sup>8</sup>). PADRIS operates under the auspices of the Agency  
106 for Health Quality and Assessment of Catalonia (“Agència de Qualitat i Avaluació Sanitàries de Catalunya”, AQUAS<sup>9</sup>). The  
107 data consist of two sets covering the period 2020-21: one providing the clinical history of individuals testing positive at least  
108 once (taken as a reference), and another with aggregated data by ABS and five-year age intervals. The latter includes details on  
109 the number of positive and negative test results, as well as information about the vaccination campaign categorized by age  
110 interval, along with specific details for nursing homes and healthcare workers.

111 Figure 2 illustrates the daily record of COVID-19 cases detected through PCR tests for the reference set. The data exhibit  
112 weekly fluctuations in the number of registered cases. These dips primarily result from reduced healthcare staffing and patients’  
113 reluctance to seek medical attention for mild symptoms during weekends, leading to lower daily case counts across Catalonia.  
114 A noteworthy aspect is a disparity of approximately 10% between the two data sets, arising from their collection from different  
115 databases and variations in anonymization criteria. We recognize this as a systematic uncertainty in our analysis.

## 116 Mobility

117 In this study, we leverage two sets of processed mobility data sourced from the INE and from the Barcelona Supercomputing  
118 Center (BSC)<sup>10</sup>. Both datasets are derived from the analysis of the same raw data, detailing the positions of 80% of mobile  
119 phones with Spanish numbers over time, offering insights into population movements. Both studies quantify mobility based on  
120 trips between origins and destinations, with a minimum duration of 2 hours for INE and 20 minutes for BSC. INE attributes  
121 weekday mobility to work activities and weekend mobility to leisure activities. In contrast, BSC captures both work and leisure

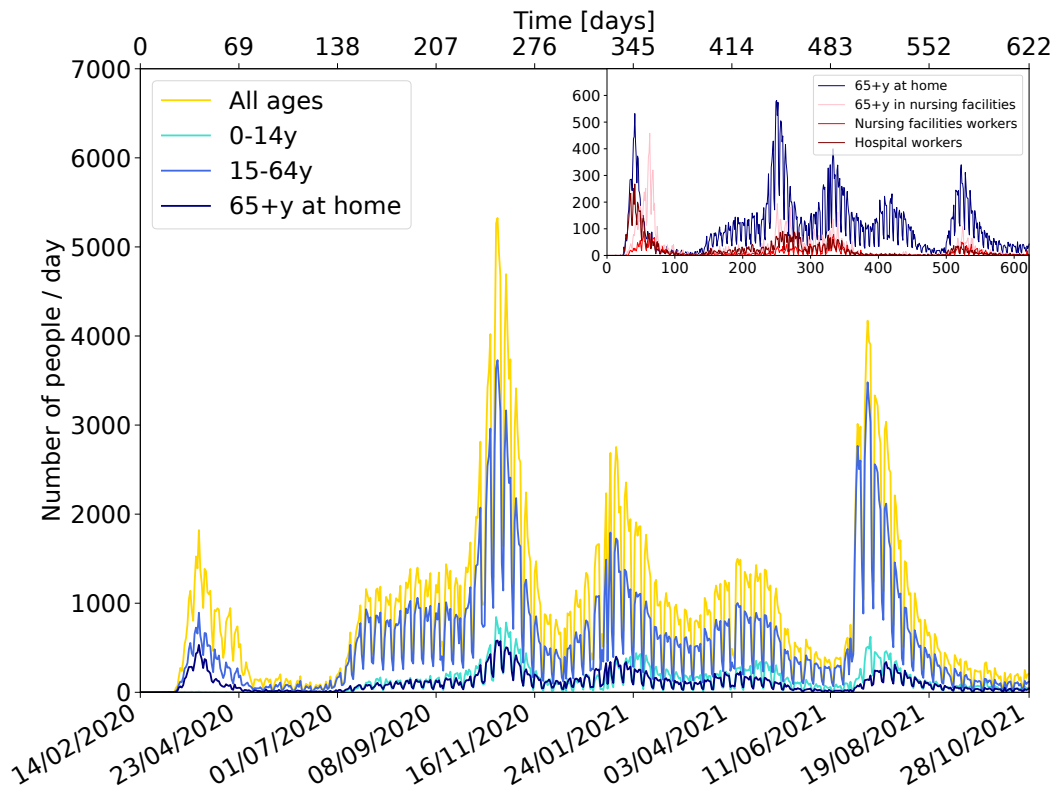


**Figure 2. COVID-19 data in Catalonia.** Total number of diagnosed people with PCR tests in Catalonia split by age categories: less than 15 years old, from 15 to 64 years old, and older (65+y) living at home. In the inset, people older than 64 years old living either at home or in nursing facilities, as well as nursing facilities and hospital workers, are shown.

122 trips during both weekdays and weekends. BSC employs a general approach to project data across different geographical layers,  
123 going from higher granularity (*mobility areas* ranging from districts to municipalities depending on the density of population)  
124 to lower granularity (such as, in order, municipalities, ABSs, provinces, etc.). The highest precision is achieved by weighting  
125 the information based on the number of inhabitants, available in the form of a 1 km<sup>2</sup> grid from GEOSTAT<sup>11</sup>. In this work we  
126 use the mobility data from the BSC projected on the ABSs and those from the INE averaged for all of Catalonia.

127 Figure 3 illustrates the weekly evolution relative to a pre-COVID-19 reference week for both sets of data aggregated  
128 over Catalonia. The mobility variation pattern is correlated between the two datasets and shows a consistent alignment with  
129 lockdown measures and holiday periods, as previously explored in our study<sup>2</sup> and discussed by BSC<sup>12</sup>. While the level of  
130 mobility is similar for work/school activities, there are notable differences in leisure activities. BSC conducted a comparative  
131 analysis of their data with that of INE<sup>10</sup>. On average, BSC reports approximately ten times more trips than INE: the difference  
132 has to be traced back to the two distinct definitions of trips previously detailed, requiring longer stays in the case of INE. The  
133 correlation remains robust, with a Pearson's coefficient close to one when aggregating over larger areas like Catalonia, but  
134 slightly diminishes to about 0.8 when comparing data from smaller geographic areas.

135 The ratio between the average daily mobility derived from BSC and INE datasets is close to one for work activities but  
136 increases to around two for leisure activities. Moreover, in correspondence with the outbreak peaks (periods characterized by  
137 stricter lockdown measures), the ratio tends to be higher, indicating a more pronounced reduction in longer trips compared  
138 to shorter ones (see SM Figure S.2). Our model incorporates mobility information in two fundamental ways: firstly, to  
139 approximate the impact of containment measures on people's contact patterns, and secondly, to delineate various population  
140 characteristics, as elucidated in the next sections. We hypothesize that a decrease in mobility corresponds to a reduction in the  
141 viral load to which individuals are exposed, although the precise effectiveness of this reduction remains uncertain. To address  
142 this uncertainty, we have introduced a calibration factor matched to data that translates the level of mobility into an estimate of  
143 the reduction in effective viral load, which in the case of leisure activities depends on the level of restrictions.

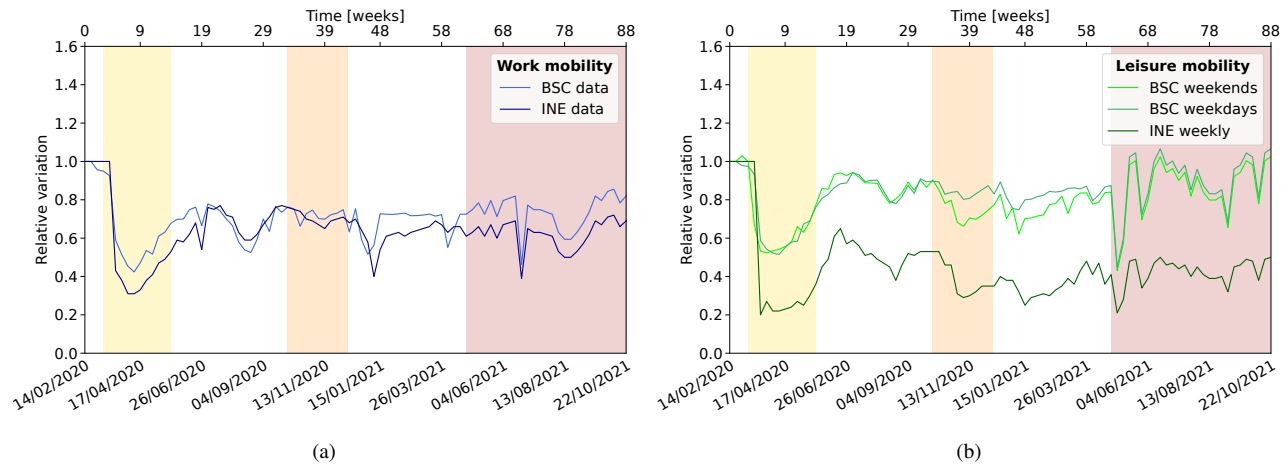


**Figure 3. Mobility Evolution.** The average daily mobility in Catalonia for (a) work/school activities and (b) leisure activities during weekdays and weekends, from INE and BSC analyses. Shaded vertical bands highlight periods of varying mobility restrictions, corresponding to the first, second, and fourth/fifth waves of the pandemic.

### Workplaces, schools, and places for leisure activities

Each member of the population is assigned a workplace or a school/university, if applicable, as well as a location for leisure activities based on their age and information obtained from the census. Census data provide insights into the occupational category of individuals, which we categorize into six sectors: primary sector, industry, construction, services, education, and healthcare. IDESCAT<sup>13</sup>, drawing from data in the “Directori central d’empreses” (DIRCE)<sup>14</sup>, furnishes details about the size and distribution of companies per sector. Schools typically consist of 30 classes of varying sizes, depending on age (0-18y) (see ref.<sup>15</sup> and table S.11). Synthetic schools are established per ABS to accommodate the corresponding number of pupils living therein. University campuses are established based on official data regarding the location and the registered number of students<sup>16</sup>. Similarly, nursing homes and hospitals are created according to their respective locations and bed capacities<sup>5,17</sup>.

We use mobility data to discern patterns of movement between different ABSs for work/school and leisure activities. For trips from home to work, we identify, for each ABS, the corresponding list of target work ABSs ranked by frequency and distance. Census data provide information on the duration it takes for individuals to commute to work (or for children to travel to school), as well as their mode of transport. This is translated into distance, and a destination ABS could be in principle chosen accordingly. In the case of work/school, we distinguish two cases: companies for which the exact ABS and size are known (e.g. universities or residencies) and those for which these data are not known. In the first case, we assign the company to workers according to distance; otherwise, we use census data to simulate a geographical distribution of businesses and educational institutions, and accommodate the list of workers of the corresponding ABS. ABSs visited for leisure activities during weekdays and weekends are allocated to single individuals based on the ABSs list provided by mobility data.

The BSC data enables monitoring of the total population residing in ABSs over time. Significant population movements are observed during the summer, with approximately 0.4 million people departing from Barcelona to visit Mediterranean coast resorts and other destinations. This is factored into the simulation, resulting in adjustments to the set of leisure contacts accordingly.

### Vaccines and vaccination campaign

In 2021, Spain launched an extensive vaccination campaign against COVID-19. The campaign commenced in January, prioritizing healthcare workers, followed by subsequent rollouts organized by age groups from oldest to youngest<sup>8,13</sup>. Participation in the vaccination drive was voluntary, and the level of uptake was notably high, exceeding 90% for individuals over 45 years of age, albeit slightly lower among younger demographics. Children under 12 were not eligible for vaccination.

The campaign administered four different vaccines belonging to two types: mRNA-based vaccines including Pfizer-BioNTech<sup>18</sup> and Moderna<sup>19</sup>, and viral-based vaccines such as AstraZeneca<sup>20</sup> and Janssen<sup>21</sup>. While the majority of individuals received mRNA-based vaccines, those in the 60-69 age group were primarily vaccinated with viral-based vaccines. The vaccination process typically involved administering a first dose followed by a second dose one month later (or two months for viral-based vaccines), followed by a booster dose six months later. Figure 4 illustrates the vaccination profile, depicting the distribution of first, second, and eventual third doses across the entire population, as well as aggregated within various age categories, according to PADRIS data.

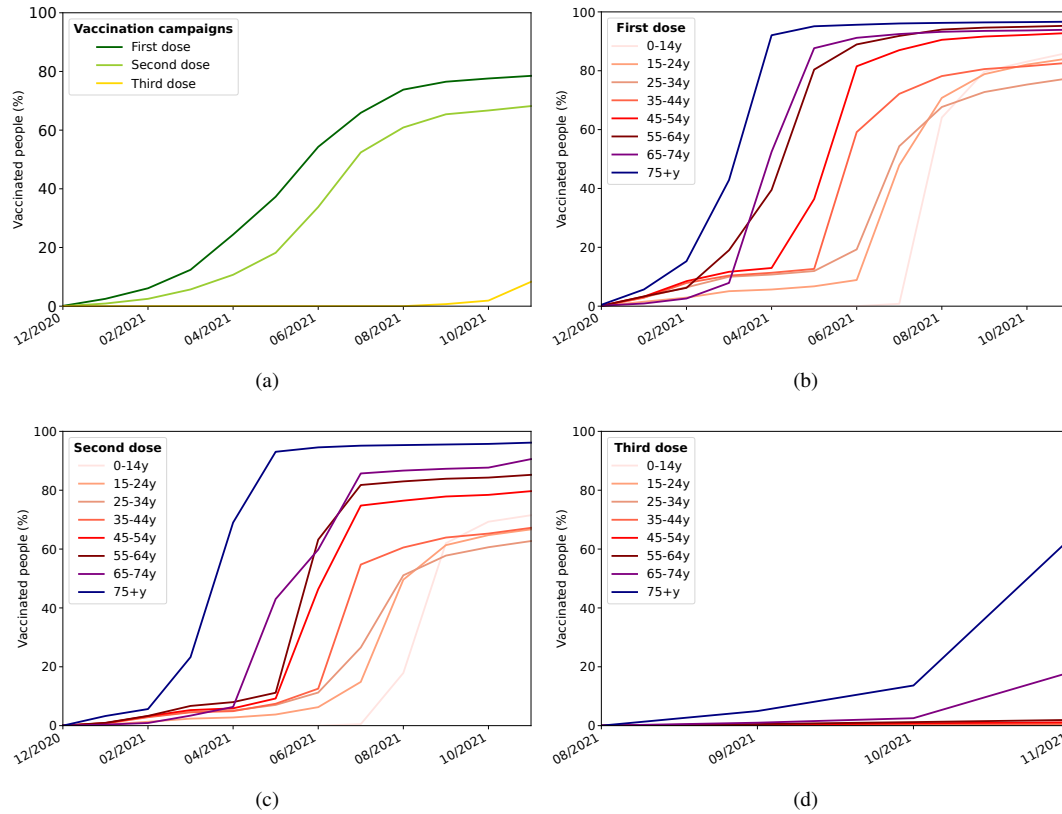


**Figure 4. 2021 vaccination campaign in Catalonia.** (a) Time profile of vaccination campaign in 2021: the first dose started to be administered in January, the second dose one month later and the third dose six months later. (b) Administration of the first dose, (c) second dose, (d) third dose, by age category.

178 The effectiveness of the vaccines is inferred from published data<sup>22</sup>. Figure 5 delineates the two effects of the vaccine  
 179 considered in the simulation: the reduction of the probability of infection and the attenuation of symptoms with a corresponding  
 180 decrease in viral load emission. For mRNA-based vaccines, the efficacy (contagion probability reduction) stands at 47% after  
 181 one dose and rises to 92% after two doses. This effectiveness remains stable for four months before gradually declining to  
 182 47% during three months. On the other hand, viral-based vaccines exhibit 40% efficacy after one dose, increasing to 76% after  
 183 two doses. This efficacy remains steady for three months before decreasing to 40% during three months. All booster doses  
 184 administered are of the mRNA type, reinstating efficacy to 92%, which remains constant throughout the simulation period.  
 185 Additionally, the reduction in viral load shedding, associated with symptom alleviation and disease severity, results in a 10%  
 186 reduction for every administered dose<sup>23</sup>.

187 Tables S.8 and S.13 in the SM provide comprehensive insights into the model for the vaccination campaign – encompassing  
 188 age categories, vaccine types, initiation dates, intervals between doses, and population coverage for each dose –, as implemented  
 189 by default in the simulation. Each age category required approximately 40 days for complete vaccination. Since details  
 190 regarding the administration of the third booster dose are lacking, we presume that individuals who received two doses  
 191 eventually received a third. This assumption underpins the simulation’s continuity and ensures a comprehensive representation  
 192 of vaccination dynamics. We have tested several scenarios, exploring diverse vaccine efficacies and timelines of administration  
 193 to assess their impact on outbreak evolution.

### 194 Model design for the COVID-19 spread

195 In our model, each individual in the population of Catalonia is assigned to one (and only one) of the following compartments at  
 196 any given time: *susceptible*, *exposed*, *infected*, *diagnosed*, *dead*, *recovered*, and *immune* (note that in our model we do not  
 197 include traditional births dynamics). When susceptible individuals come into contact with infected persons, their state may  
 198 transition to exposed based on the probability

$$P = 1 - e^{-\lambda_i \cdot F_i^{\text{EfficiencyVaccine}}(t) \cdot \Delta t} \quad (1)$$

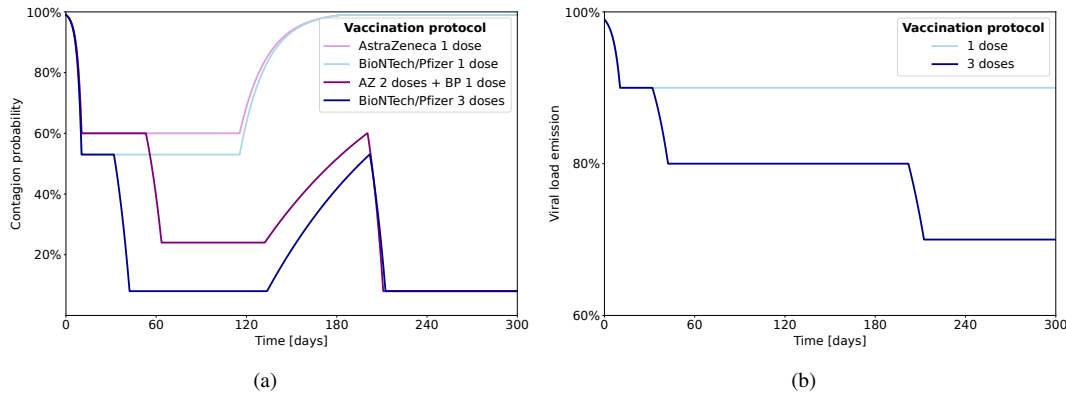


**Figure 5. Effects of vaccine.** The vaccine has two effects: **(a)** Reduction of contagion probability due to vaccine. The reduction of probability of becoming infected is shown for two cases: a single dose of vaccine, and three doses of vaccines for Pfizer/Moderna and AstraZeneca/Janssens. **(b)** Moderation of the infectious process with the corresponding reduction of viral load emission.

199 Here, the force of infection,  $\lambda_i$ , represents the total viral load a *single individual i* is exposed to per unit time (day).  
 200  $F_{\text{Efficiency Vaccine}}^i(t)$  denotes the reduction in the risk of infection resulting from vaccination, and  $\Delta t$  is the time interval (1/3 day).  
 201 A comprehensive mathematical description of the estimate of  $\lambda_i$  is given in Section 2.1 of the SM. Here we will limit the  
 202 discussion to a general description of the computational strategy.

203 The total viral load exposure  $\lambda_i$  is a composite of exposures occurring throughout the day across various settings. It  
 204 primarily encompasses contributions from three distinct eight-hour intervals corresponding to an individual's time spent at  
 205 home, work, or school, and engaging in social activities. To compute  $\lambda_i$ , we calculate the viral load emitted by every individual  
 206 and multiply by matrices describing the network of contacts. Additional contributions are considered for individuals using  
 207 public transportation or visiting particularly crowded areas during their daily routines (for example, tourist areas during summer,  
 208 or commercial areas during season holidays). In that case, to compute  $\lambda_i$ , we estimate the average viral shedding of people  
 209 involved in these activities or encountered within these settings, modulated by ABS-dependent mobility. We then multiply by  
 210 the number of estimated contacts, e.g. during a typical trip in public transport, or the number of additional contacts during  
 211 leisure activities (the latter are ABS-dependent and typically higher in summer coastal resorts or tourist areas of Barcelona).  
 212 Details about relative contributions are given in Section 5 of the SM.

213 After the exposure, our population model considers personalized disease progression for each individual, with characteristics  
 214 such as age-dependent symptoms and viral shedding levels (a survey of the epidemiological data used in the model is available in  
 215 a previous publication<sup>2</sup>). These factors influence other outcomes, such as the likelihood of diagnosis or hospitalization. Infected  
 216 individuals are classified based on symptoms (symptomatic or asymptomatic) and viral shedding intensity (strongly infectious,  
 217 moderately infectious, or non-infectious). Three key combinations emerge: asymptomatic non-infectious (ANI), asymptomatic  
 218 moderately infectious (AMI), and symptomatic strongly infectious (SSI). Age plays a crucial role, with older individuals more  
 219 likely to exhibit symptoms and higher infectiousness, while children tend to be ANI. Additionally, symptomatic individuals are  
 220 typically twice as infectious as asymptomatic ones. The overall infectiousness level is set for every individual according to  
 221 these categories.

222 The model also incorporates probabilities of hospitalization and intensive care unit (ICU) admission, which correlate  
 223 with symptom intensity. However, detailed temporal dynamics post-diagnosis, including hospitalization progression, are not  
 224 explicitly modelled. Upon diagnosis, a portion of the population is tagged as hospitalized or in ICUs. Death can occur regardless  
 225 of diagnosis or hospitalization, while recovery follows a fixed time frame unless death intervenes. Recovered individuals are  
 226 considered immune against further infection for an average of nine months, with a root mean square (RMS) deviation of three  
 227 months. In the case of a reinfection, their viral load emission is reduced (see Table S.6).

## 228 Model Calibration

229 Our simulation model is constructed upon 194 parameters to account for the population description, the disease characteristics,  
 230 the modelling of contacts, and the vaccination campaign (see Section 6 of the SM for a compilation). Most of the parameters can  
 231 be set *a priori* from existing data (see Subsection 3.1 in the SM). Nevertheless, given that some of them are poorly known and  
 232 difficult to determine precisely only from this comparison, we study the individual sensitivity of the model to each parameter  
 233 and further calibrate the model via a goodness-of-fit test algorithm.

234 Ideally, to reproduce more accurately the observed evolution of diagnosed people, a simultaneous fit of all parameters  
235 should be performed (cf. Subsection 3.3 of the SM). However, this would require a complete modelling of the correlations  
236 between all parameters, with their respective ranges of variation, for which there is not enough knowledge. We follow instead  
237 an approximate procedure, concentrating on the most sensitive parameters. The fits are done successively one at a time with  
238 their respective systematic and statistical uncertainties. The cost function for each parameter is based on a  $\chi^2$  statistic.

239 Only the three most sensitive parameters – broadly affecting age, spatial and time dependence – are calibrated using  
240 this procedure; in decreasing order of sensitivity, these are related to the mobility of people for leisure activities, the global  
241 infectiousness of the virus, and the relative weight of this infectiousness across different age groups. The calibrations are  
242 performed over the first year of the evolution of the disease, before the data and model are directly influenced by the active  
243 vaccination campaign. Additionally, due to shortcomings in the real-life data collection process, it is not possible to perform  
244 comparisons on a daily basis; instead, data has to be aggregated on a weekly basis, taken from Friday to Thursday to account  
245 for delayed registers. Further details on these considerations and the calibration process can be found in Section 3 of the SM.  
246 We estimate a minimum of 10% relative uncertainty to be associated with the calibration of these three parameters, which is  
247 represented in the figures by a shaded area. This does not include the uncertainty that may originate from imperfect knowledge  
248 of the other parameters.

## 249 Results

### 250 The natural history of COVID-19 in Catalonia

251 Figure 6 shows the results of our simulation after the model calibration process, extended to the full two-year evolution and  
252 compared against the collected data, aggregated across all provinces and age groups. The results span from February 14, 2020,  
253 to the end of October 2021, the period with consistent data availability.

254 During 2020, Catalonia experienced two distinct waves. An initial wave in March, whose shape is influenced by the specific  
255 characteristics of the disease and the mobility trends. Among these factors, the force of infection, pre-symptomatic viral  
256 shedding, and disease duration stand out, as well as changes in mobility patterns and the gradual recovery of work-related  
257 mobility. Thanks to the strict lockdown measures implemented, this initial outbreak was mitigated, and it was followed by a  
258 plateau. The summer plateau's level and shape are linked to post-lockdown contacts, especially summer activities, and their  
259 timing. As lockdown restrictions eased and activities resumed — partially at first, then almost fully — after the summer, the  
260 increase in disease incidence at the end of this season prompted the emergence of a second wave in October. This latter wave  
261 was effectively curtailed by ad-hoc lockdown measures.

262 In 2021, the vaccination campaign played a crucial role in managing subsequent waves, although three additional waves  
263 were observed, each triggered by social gatherings during holiday periods: Christmas, Easter break, and summer holidays.  
264 These waves, including those in January 2021, are similarly shaped by changes in contacts, with the impacts of the vaccination  
265 campaign becoming increasingly apparent.

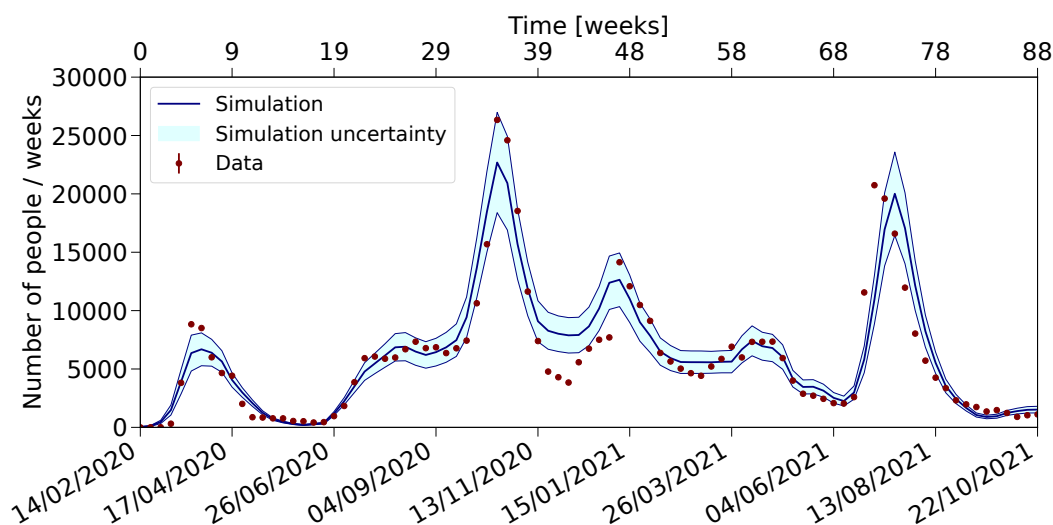


**Figure 6. Number of diagnosed people in Catalonia.** Data on diagnosed people are compared to simulation results for the period from 2020 to 2021.



266 The analysis of the different components of the viral load  $\lambda_i$  (see SM Fig S.15) shows that the contribution from “home”  
267 dominates, especially in the periods of strong confinement. In the periods of more mobility, the “leisure” contacts are the  
268 second most relevant, followed by “work” activities.

269 Similar results for more specific subgroups (children, adults, seniors, nursing home residents and workers, and hospital  
270 workers) are presented in the SM (see Figs. S.5-S.10), highlighting differences in symptomatology and testing patterns across  
271 waves. Children are mostly asymptomatic, while old people are mostly strongly infectious. During the first wave only people  
272 with strong symptoms were tested, so very few children were diagnosed. Later on, a broader spectrum of people were tested,  
273 including close contacts of diagnosed people.

274 We also compare our model against data aggregated by provinces (SM, Figs. S.11-S.14). The Barcelona province, hosting  
275 the largest fraction of the population and with the strongest statistical power in the fit, is well reproduced in the simulation,  
276 along with the main features of the other less populated provinces. All three provinces exhibit essentially the same five waves  
277 as Barcelona, albeit with some differences in relative intensity. Notably, the summer 2020 “plateau” observed in Barcelona is  
278 absent in Girona and Tarragona, where a more gradual increase is observed. Additionally, Lleida featured an additional strong  
279 wave in July 2020 associated with the influx of temporary workers in the agricultural sector. The correlation between the daily  
280 evolution of waves in different provinces provides insights into their nature, as previously discussed<sup>24</sup>. Pearson’s correlation  
281 coefficients between diagnosed cases in the four provinces during the March and October waves exhibit a high degree of  
282 correlation, reflecting the synchronous spread of the virus (SM, Table S.4). However, during the summer period, characterized  
283 by increased holiday activities and foreign visitors, correlations are weaker, and in the case of Lleida, even negative due to  
284 specific local factors such as the influx of temporary workers in agriculture. The simulation generally reproduces the observed  
285 correlation patterns, indicating its capability to capture the essential features of disease spread within the Catalan territory.

286 Estimates of contacts across provincial borders during leisure activities reveal higher exchange rates between Barcelona and  
287 its neighbours (see Table S.5 of the SM). This exchange disproportionately affects less populated provinces, with significant  
288 impacts during summer as residents from Barcelona (about 400k people) travel to Mediterranean coastal resorts and the  
289 Pyrenees region. The relative impact in the provinces of Girona, Tarragona, and Lleida is 30, 20, and 10%, respectively.  
290 This effect is incorporated into the simulation, virtually reallocating part of the population in different ABSs during summer,  
291 which also implies changing the list of potential contacts. In any case, the tendency for the simulation to overestimate disease  
292 incidence in the outer provinces is possibly due to assumptions about contact patterns not fully accounting for differences in  
293 population density.

## 294 **The 2021 vaccination campaign**

295 The prompt start of the vaccination campaign in 2021, along with its age-dependent profile and high level of participation,  
296 played pivotal roles in controlling the virus’s spread, limiting the number of infected cases, and facilitating the relaxation of  
297 containment measures to revive economic activities (details of the modelling of the vaccination campaign are collected in  
298 Table S.13 of the SM). Figure 7 demonstrates the significant impact of the vaccine campaign: in particular, the number of  
299 diagnosed cases, which would have shown a high peak during the summer if no vaccination measures were implemented, was  
300 instead reduced to a manageable level even while mobility was at its highest. The timeliness of the campaign was crucial,  
301 as a delay of three months would not have entirely prevented the summer peak but would only have decreased its severity.  
302 Such a scenario would likely have required the enforcement of stringent lockdown policies, with an adverse impact on society.  
303 Thus, vaccination emerged as a crucial component in the journey back to “normality”. We explored a scenario where vaccine  
304 effectiveness was reduced and assumed all vaccines administered were the same, with a 76% reduction in the probability of  
305 infection. This situation led to three times more diagnosed cases, underscoring the importance of vaccine efficacy in controlling  
306 disease transmission.

## 307 **Data limitations**

308 While the census data provide a detailed description of the population, including home composition, unavoidable simplifications  
309 arise due to data limitations. First, and more importantly, the reliability of the recorded number of positive cases is severely  
310 mined by under-reporting<sup>25–27</sup> (for both infections and deaths). In the second instance, mobility data obtained from mobile  
311 phones lack age information and do not offer objective insights into age group differences. Furthermore, while mobile phone  
312 traffic provides geographic displacement data both for leisure and work-related activities, information regarding workplace  
313 size, location, and company type was unavailable at the desired granularity. Nonetheless, our analysis highlights the timely  
314 implementation of containment measures and vaccination campaigns by authorities as crucial factors in controlling epidemics.

## 315 **Conclusions**

316 We have developed an advanced agent-based simulation model tailored to accurately reproduce the dynamics of COVID-19  
317 spread in Catalonia throughout 2020 and 2021. This comprehensive simulation encompasses all the essential ingredients

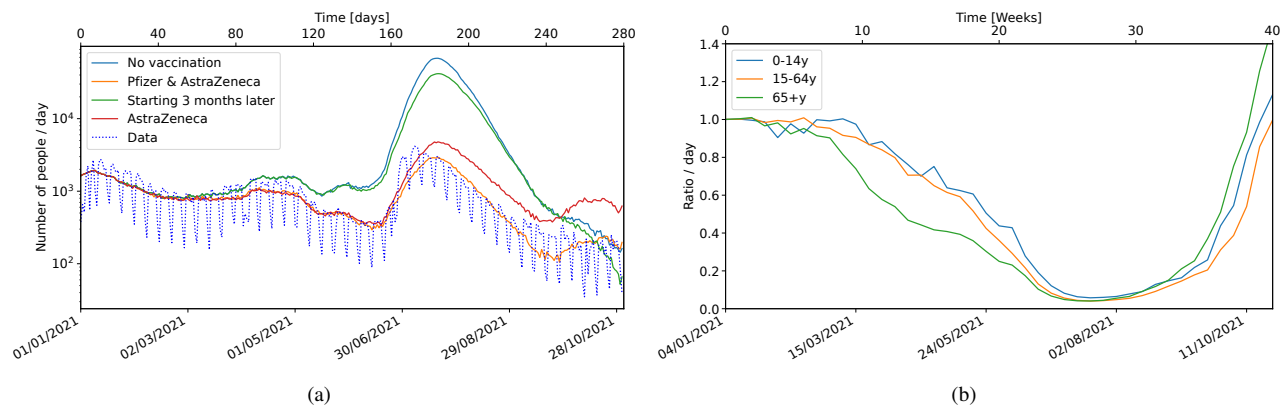


**Figure 7. Diagnosed people for different vaccination scenarios.** **a** Number of diagnosed people in 2021 in a no-vaccination scenario compared with different vaccination campaigns, including the actual campaign implemented in Catalonia. **b** Ratio of the number of diagnosed people in 2021 with and without vaccination for the vaccination campaign implemented in Catalonia for different age categories. The 15-64y category includes hospital and residency workers, and the 65+y includes residents in nursing homes.

318 with enough precision to reproduce the flows of the pandemic across various age groups and provinces over the entire period  
319 under study. Our approach relies on high-quality disaggregated data, and not only provides valuable insights into spatial  
320 autocorrelation concerning the COVID-19 incidence during different phases of the outbreak but also estimates the impact of  
321 external interventions on human behaviour.

322 Several strengths of our method are worth highlighting. First and more importantly, our use of a granular representation of  
323 the population: the consistent availability of mobility, census, and health data at relatively small spatial units (ABSs) makes  
324 possible a robust calibration and comparison with real-world data, allowing for the discovery of important factors causing  
325 disease transmission; our agent-based model avoids the drawbacks of averaging population characteristics over broad regions  
326 and provides a more realistic description of local dynamics. Accurate modelling of contact patterns is ensured by the granularity  
327 of mobility data, which takes into consideration seasonal fluctuations and their impact on the virus spread. In this way, we  
328 are able to successfully capture both the effects of varied lockdown measures across different regions and the movements of  
329 populations with high temporal and spatial resolution.

330 The combination of health data with our model provides also a faithful replica of the age- and time-dependent vaccination  
331 campaign, which is a crucial aspect for understanding changes in the population behaviour that occur during the second year of  
332 the outbreak. The model can be easily expanded to include additional (epidemiological and etiological) virus characteristics,  
333 as well as demographic factors. Furthermore, although initially developed for Catalonia, our simulator can be adjusted for  
334 analysing other contexts at different geographical scales, upon the availability of high-quality data.

335 In conclusion, thanks to its accuracy, our model can serve as a reliable tool for assessing the efficacy of containment  
336 measures (in particular at a local scale) and providing invaluable insights to delineate targeted public health strategies.

## 337 References

- 338 1. Silverman, E. *et al.* Situating agent-based modelling in population health research. *Emerg. Themes Epidemiol.* **18**, DOI:  
339 [10.1186/s12982-021-00102-7](https://doi.org/10.1186/s12982-021-00102-7) (2021).
- 340 2. Bosman, M. *et al.* Stochastic simulation of successive waves of COVID-19 in the province of barcelona. *Infect. Dis. Model.*  
341 **8**, 145–158, DOI: <https://doi.org/10.1016/j.idm.2022.12.005> (2023).
- 342 3. CatSalut. Servei Català de la Salut. <https://catsalut.gencat.cat/ca/inici/>.
- 343 4. INE. Instituto Nacional de Estadística. <https://www.ine.es/>.
- 344 5. ERCCHyS. Centro de Ciencias Humanas y Sociales, CSIC. Envejecimiento en Red, datos de abril de 2019. [http://](http://envejecimiento.csic.es/documentos/documentos/enred-estadisticasresidencias2019.pdf)  
345 [envejecimiento.csic.es/documentos/documentos/enred-estadisticasresidencias2019.pdf](http://envejecimiento.csic.es/documentos/documentos/enred-estadisticasresidencias2019.pdf).
- 346 6. EnR. Instituto Nacional de Estadística (INE). Una estimación de la población que vive en residencias de mayores.  
347 <http://envejecimientoenred.es/una-estimacion-de-la-poblacion-que-vive-en-residencias-de-mayores/>.
- 348 7. DIBA. Diputació de Barcelona. Informació Estadística Local. <https://www.diba.cat/hg2/presentacioprov.asp?prid=954>.

- 349 **8.** PADRIS. Programa d'Analítica de Dades per a la Recerca i la Innovació en Salut. <https://aquas.gencat.cat/ca/detall/article/padri>.
- 350
- 351 **9.** AQuAS. Agència de Qualitat i Avaluació Sanitàries de Catalunya. <https://aquas.gencat.cat/ca/actualitat/ultimes-dades-coronavirus/>.
- 352
- 353 **10.** Ponce-de Leon, M. *et al.* COVID-19 flow-maps an open geographic information system on COVID-19 and human mobility for spain. *Sci. Data* **8**, DOI: [10.1038/s41597-021-01093-5](https://doi.org/10.1038/s41597-021-01093-5) (2021).
- 354
- 355 **11.** European Forum for GeoStatistics. Essnet project geostat 1a-representing census data in a european population grid-final report. <https://www.efgs.info/wp-content/uploads/geostat/1a/GEOSTAT1A-final-report.pdf>.
- 356
- 357 **12.** Smith, M., Ponce-de Leon, M. & Valencia, A. Evaluating the policy of closing bars and restaurants in Cataluña and its effects on mobility and COVID-19 incidence. *Sci. Reports* **12**, DOI: [10.1038/s41598-022-11531-y](https://doi.org/10.1038/s41598-022-11531-y) (2022).
- 358
- 359 **13.** IDESCAT. Statistical Institute of Catalonia. <https://www.idescat.cat/>.
- 360 **14.** DIRCE. Directorio Central de Empresas. <https://www.ine.es/dynt3/inebase/es/index.htm?padre=51&dh=1>.
- 361 **15.** Departament d'Ensenyament - Generalitat de Catalunya. Ràtios d'alumnes per estudi i unitat o grup. <https://educacio.gencat.cat/ca/departament/estadistiques/indicadors/sistema-educatiu/escolaritzacio/ratios/>.
- 362
- 363 **16.** Universitats catalanes. <https://universitats.gencat.cat/ca/estudis-universitaris/universitats-catalanes/>.
- 364 **17.** Centres i llits hospitalaris. Comarques i Aran, i províncies. <https://www.idescat.cat/indicadors/?id=aec&n=15808>.
- 365 **18.** Pfizer-BioNTech COVID-19 Vaccine. . <https://www.pfizer.com/products/product-detail/pfizer-biontech-covid-19-vaccine>.
- 366 **19.** Moderna COVID-19 Vaccine (2023-2024 Formula). <https://eua.modernatx.com/>.
- 367 **20.** AstraZeneca COVID-19 Vaccine. <https://www.azcovid-19.com/>.
- 368 **21.** Janssens COVID-19 Vaccine. <https://www.janssen.com/COVID19/>.
- 369 **22.** Comparison-of-covid-19-vaccines, and references therein. <https://myacare.com/blog/comparison-of-covid-19-vaccines>.
- 370 **23.** Tan, S. *et al.* Infectiousness of SARS-CoV-2 breakthrough infections and reinfections during the Omicron wave. *Nat. Medicine* **29**, 358 – 365, DOI: [10.1038/s41591-022-02138-x](https://doi.org/10.1038/s41591-022-02138-x) (2023).
- 371
- 372 **24.** Belvis, F. *et al.* Key epidemiological indicators and spatial autocorrelation patterns across five waves of COVID-19 in Catalonia. *Sci. Reports* **13**, DOI: [10.1038/s41598-023-36169-2](https://doi.org/10.1038/s41598-023-36169-2) (2023).
- 373
- 374 **25.** Moriña, D. *et al.* Cumulated burden of COVID-19 in Spain from a Bayesian perspective. *Eur. J. Public Heal.* **31**, 917 – 920, DOI: [10.1093/eurpub/ckab118](https://doi.org/10.1093/eurpub/ckab118) (2021).
- 375
- 376 **26.** Moriña, D., Fernández-Fontelo, A., Cabaña, A., Arratia, A. & Puig, P. Estimated Covid-19 burden in Spain: ARCH underreported non-stationary time series. *BMC Med. Res. Methodol.* **23**, DOI: [10.1186/s12874-023-01894-9](https://doi.org/10.1186/s12874-023-01894-9) (2023).
- 377
- 378 **27.** Garcia-Carretero, R., Vazquez-Gomez, O., Gil-Prieto, R. & Gil-de Miguel, A. Hospitalization burden and epidemiology of the COVID-19 pandemic in Spain (2020–2021). *BMC Infect. Dis.* **23**, DOI: [10.1186/s12879-023-08454-y](https://doi.org/10.1186/s12879-023-08454-y) (2023).
- 379
- 380 **28.** INE. Estudios de movilidad a partir de la telefonía móvil. [https://www.ine.es/experimental/movilidad/experimental\\_em.htm](https://www.ine.es/experimental/movilidad/experimental_em.htm).
- 381 **29.** Ferguson, N. *et al.* Report 9: Impact of non-pharmaceutical interventions (npis) to reduce COVID-19 mortality and healthcare demand. *Imperial College COVID-19 Response Team* DOI: [10.25561/77482](https://doi.org/10.25561/77482) (2020).
- 382
- 383 **30.** NetworkX, Python package for the creation, manipulation, and study of the structure, dynamics, and functions of complex networks. <https://networkx.org/>.
- 384
- 385 **31.** Hakimi, S. L. On realizability of a set of integers as degrees of the vertices of a linear graph. I. *J. Soc. for Ind. Appl. Math.* **10**, 496–506, DOI: [10.1137/0110037](https://doi.org/10.1137/0110037) (1962).
- 386
- 387 **32.** Newman, M. E. J. The structure and function of complex networks. *J. Soc. for Ind. Appl. Math.* **45**, 167–256, DOI: [10.1137/S003614450342480](https://doi.org/10.1137/S003614450342480) (2003).
- 388
- 389 **33.** Prem, K. *et al.* Projecting contact matrices in 177 geographical regions: An update and comparison with empirical data for the COVID-19 era. *PLoS Comput. Biol.* **17**, 1DUMMUY, DOI: [10.1371/journal.pcbi.1009098](https://doi.org/10.1371/journal.pcbi.1009098) (2021).
- 390
- 391 **34.** Bi, Q. *et al.* Epidemiology and transmission of COVID-19 in 391 cases and 1286 of their close contacts in Shenzhen, China: a retrospective cohort study. *The Lancet Infect. Dis.* **20**, 911 – 919, DOI: [10.1016/S1473-3099\(20\)30287-5](https://doi.org/10.1016/S1473-3099(20)30287-5) (2020).
- 392
- 393 **35.** He, X. *et al.* Temporal dynamics in viral shedding and transmissibility of COVID-19. *Nat. Medicine* **26**, 672–675, DOI: [10.1038/s41591-020-0869-5](https://doi.org/10.1038/s41591-020-0869-5) (2020).
- 394

- 395 **36.** Di Domenico, L., Pullano, G., Sabbatini, C. E., Boëlle, P.-Y. & Colizza, V. Impact of lockdown on COVID-19 epidemic in  
396 Île-de-France and possible exit strategies. *BMC Medicine* **18**, DOI: [10.1186/s12916-020-01698-4](https://doi.org/10.1186/s12916-020-01698-4) (2020).
- 397 **37.** Instituto de Salud Carlos III. Anàlisi de los casos de COVID-19 notificados a la RENAVE hasta el 10 de  
398 mayo en España. Informe COVID-19 n° 33. 29 de mayo de 2020. [https://www.isciii.es/QueHacemos/Servicios/  
399 VigilanciaSaludPublicaRENAVE/EnfermedadesTransmisibles/Paginas/-COVID-19.-Informes-previos.aspx](https://www.isciii.es/QueHacemos/Servicios/VigilanciaSaludPublicaRENAVE/EnfermedadesTransmisibles/Paginas/-COVID-19.-Informes-previos.aspx).
- 400 **38.** Tolossa, T. *et al.* Time to recovery from COVID-19 and its predictors among patients admitted to treatment center of  
401 Wollega University Referral Hospital (WURH), Western Ethiopia: Survival analysis of retrospective cohort study. *PLoS*  
402 *ONE* **16**, DOI: [10.1371/journal.pone.0252389](https://doi.org/10.1371/journal.pone.0252389) (2021).
- 403 **39.** AMT. Enquesta de Mobilitat en Dia Feiner (EMEF) - 2019. [https://www.atm.cat/web/es/observatori/  
404 encuestas-de-movilidad.php](https://www.atm.cat/web/es/observatori/encuestas-de-movilidad.php).
- 405 **40.** GenCat. Diari Oficial de la Generalitat de Catalunya. <https://dogc.gencat.cat/ca/inici/>.
- 406 **41.** Cheng, Y. *et al.* Face masks effectively limit the probability of SARS-CoV-2 transmission. *Science* **372**, 1339–1343, DOI:  
407 [10.1126/science.abg6296](https://doi.org/10.1126/science.abg6296) (2021).
- 408 **42.** Wang, Y., Deng, Z. & Shi, D. How effective is a mask in preventing COVID-19 infection? *Med. devices & sensors* **4**,  
409 e10163, DOI: [10.1002/mds3.10163](https://doi.org/10.1002/mds3.10163) (2021).

## 410 Acknowledgements

411 The authors affiliated to CED, IFAE and i2CAT acknowledge the support of the CERCA institution, Centres de Recerca de  
412 Catalunya. They acknowledge the support of the “Agència de Gestió d’Ajuts Universitaris i de Recerca” (AGAUR) via the grant  
413 PANDE00180 “A powerful stochastic tool to assess the impact of the COVID-19 in Catalonia integrating detailed demographic  
414 and mobility data” of the program PANDÈMIES 2020 “Replegar-se per créixer: l’impacte de les pandèmies en un món sense  
415 fronteres visibles”. The grant funded the work of YC, AO and (partially) of AM. The authors acknowledge the support of  
416 PADRIS (“Programa d’Analítica de Dades per a la Recerca i la Innovació en Salut”) operating under the auspices of AQuAS  
417 (“Agència de Qualitat i Avaluació Sanitàries de Catalunya”) for providing the health data. They acknowledge the help of Albert  
418 Esteve from CED-CERCA in obtaining the PADRIS and Census data.

419 The work of VV has been partially funded by Next Generation EU through the project “GeTOnQuaM”. The research  
420 activities of CGP and VV have been carried out in the framework of the INFN Research Project QGSKY. VV extends his  
421 appreciation to the Italian National Group of Mathematical Physics (GNFM, INdAM) for its support.

## 422 Author contributions statement

423 MB led the conception of the project. YC, MD, LG, CG, MM, LLM, PM, AO and VV contributed to the modelling design.  
424 MB, YC, AM, AO took care of data preparation. MB, YC, MD, LG, CG, MM, LLM, AO developed the code. MB, PM, CG,  
425 LLM, VV wrote the manuscript. All authors contributed to the discussion and interpretation of the results, revised critically the  
426 draft and approved the final version of the manuscript.

## 427 Additional information

428 The authors declare no competing interests.

## 429 Data availability

430 The population census, was provided by the Spanish National Statistics Institute (Instituto Nacional de Estadística, INE). The  
431 health data were provided by PADRIS (“Programa d’Analítica de Dades per a la Recerca i la Innovació en Salut”) operating under  
432 the auspices of AQuAS (“Agència de Qualitat i Avaluació Sanitàries de Catalunya”). In compliance with European and national  
433 laws, the above datasets were only made available to the researchers participating in this study and cannot be shared by them with  
434 other parties. Researchers can request census data from INE at <https://www.ine.es/ProductsAndServices/StatsticalInformation.cat>,  
435 and from AQuAs by contacting PADRIS at [padris@gencat.cat](mailto:padris@gencat.cat). The sets of processed mobility data are publicly available from  
436 INE at <https://www.ine.es/experimental/movilidad/>, and from BSC at <https://github.com/bsc-flowmaps>. Data sets generated  
437 during the current study are available from the corresponding author on reasonable request.